# Quantum Experiments and Graphs II:
# Computation and State Generation with Probabilistic Sources and Linear Optics

Xuemei Gu,[1, 2, *] Mario Krenn,[1, 3, †] Manuel Erhard,[1, 3] and Anton Zeilinger[1, 3, ‡]

[1]*Institute for Quantum Optics and Quantum Information (IQOQI),*
*Austrian Academy of Sciences, Boltzmanngasse 3, 1090 Vienna, Austria.*
[2]*State Key Laboratory for Novel Software Technology, Nanjing University,*
*163 Xianlin Avenue, Qixia District, 210023, Nanjing City, China.*
[3]*Vienna Center for Quantum Science & Technology (VCQ), Faculty of Physics,*
*University of Vienna, Boltzmanngasse 5, 1090 Vienna, Austria.*

(Dated: April 2, 2018)

We show how general linear optical quantum entanglement experiments with probabilistic sources can be described using graph theory. By introducing complex weights in undirected graphs, we can naturally work with quantum superpositions. This immediately leads to many interesting results, some of which we present here. Firstly, we identify a conceptually new and experimentally completely unexplored method to solve classically intractable problems with quantum experiments. The problem is in the complexity class #P-COMPLETE, and deals with the computation of a generalization of the matrix function *Permanent*. Second, we show that a recent no-go result applies generally to linear optical quantum experiments, thus revealing important insights to quantum state generation with current photonic technology. Third, we show how to easily understand in a graphical way quantum experiments such as entanglement swapping. This connection offers a novel perspective on a widely used technology, and immediately raises many new questions.

Photonic quantum experiments prominently use probabilistic photon sources in combination with linear optics [1]. This allows for the generation of multipartite quantum entanglement (such as GHZ states [2–5], W states [6], Dicke states [7, 8] or high-dimensional states [9, 10]), proof-of-principle experiments of special-purpose quantum computing [11–16] or applications such as quantum teleportation [17, 18] and entanglement swapping [19, 20].

Here we show that one can describe all of these quantum experiments with graphs. To do this, we generalize a recently found link between graphs and special quantum experiments [21] – which were based on the computer-inspired concept of *Entanglement by Path Identity* [22, 23]. By using complex weighted graphs and realising that linear optical elements stay within the graph description, we can naturally describe quantum superposition and quantum interference for general linear optical quantum experiments. This technique enables us to find several results: (1) We identify a novel scheme to experimentally simulate a classically very difficult problem which is in the complexity class #P-COMPLETE – namely the calculation of the number of perfect matchings in a general graph. The experimental scheme works via multiphotonic generalisation of frustrated pair-creation[1]. While the two-photon interference effect has been been observed

more than 20 years ago [24], the multi-photon generalisation has never been investigated experimentally. (2) We show that insights from graph theory identify restrictions on the possibility of realizing certain classes of entangled states with current photonic technology. (3) The graph-theoretical description of experiments also leads to an intuitive pictorial explanation of quantum protocols such as entanglement swapping.

*Linear Optical Experiments and Graphs* — As a warm-up example, we show a method to experimentally generate a GHZ state and its description as a graph in Fig.1A. There, each vertex represents a photon path and each edge stands for a non-linear crystal which can probabilistically produce a photon pair. The final state is obtained under the condition of four-fold coincidences, which means that all four detectors click simultaneously. In the graph, this corresponds to a *perfect matching* – a subset of edges that contains every vertex exactly once. The resulting quantum state is a coherent superposition of perfect matchings of the graph.

Now that we have familiarized ourselves with the description of experiments by use of graphs, we are ready to apply it to linear optics. For this we describe first the action of a beam splitter, one of the key elements in photonic quantum experiments, in Fig.1B. Analogous to Fig.1A, each vertex represents a photon path and each edge a photon pair correlation. An incoming photon into a BS has two possibilities: it can be reflected or transmitted. These two possibilities are represented in the graph by a doubling of the original edge: One edge replaces the original edge (in the case of reflection), with the weight being multiplied by a phase of $\pi/2$. In the second edge, the vertex of the

---

[1] Frustrated pair-creation is an effect where the amplitudes of two pair-creation events can construtively or destructively interfere
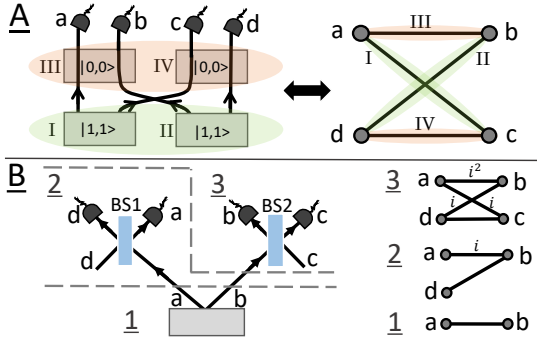
Figure 1. Linear optical experiments and Graphs. **A**: We take an optical setup as example, which produces a 2-dimensional 4-photon GHZ-state with the method presented in *Entanglement by Path Identity* [23]. When the crystals I-IV are pumped coherently and two of them produce photon pairs, a photon in each detector *a-d* can only occure when crystal I-II (each producing $|1,1\rangle$) or III-IV (with $|0,0\rangle$)produce a pair each. All other combinations (like I and III) do not lead to 4-fold coincidences. This results in a 4-particle GHZ state. The setup can be described with a graph [21] which is shown on the right side. Each vertex represents a photon path and each edge one crystal. The final output state is computed by *perfect matchings* (a subset of edges which contains every vertex exactly once). **B**: An example of linear optical setup with one crystal, two 50:50 beam splitters (BSs) and four detectors. The corresponding graph is depicted on the right side. Again, every vertex represents one photon path and each edge a photon pair correlation. Step **1**: A crystal produces a photon pair in path *a* and *b*. Therefore the corresponding graph has an edge between vertex *a* and *b*. Step **2**: The photon in path *a* propagates to BS1 which will reflect to path *a* and transmit to path *d*. The corresponding operation in the graph is doubling the original edge $E_{ab}$ to $E_{db}$ while $E_{ab}$ gets a complex weight $i$. We call this manipulation *BS operation*. Step **3**: The photon in path *b* propagates to BS2 which will reflect to path *b* and transmit to path *c*. As in step **2**, all edges connected with vertex *b* ($E_{ab}$, $E_{db}$) are doubled to edges connected with vertex *c* ($E_{ac}$, $E_{cd}$) while the original weighted edges get an additional complex weight $i$. We thus get the corresponding graph of the setup. Calculating the perfect matchings leads to four-fold coincidence counts.



Figure 2. Quantum interference and Graphs. **A**: An optical setup for Hong-Ou-Mandel (HOM) interference. A crystal generates a photon pair in paths *a* and *b* which propagate to a 50:50 BS. The photon in path *a* will reflect to path *a* and transmit to path *b*, the photon in path *b* propagates in a similar way. The right side shows the corresponding graph. The small light-gray disks with labels indicate the mode property of a photon, for example the polarization. All modes of a photon in one path (depicted with a large gray disk) form one *vertex set*. By using the *BS operation*, we get the final graph. The weights $i$ and $i^2$ are corresponding to phases $\frac{\pi}{2}$ and $\pi$ and are depicted in different colors. Now let's look at the two cases where the photons are indistinguishable or distinguishable. **B**: For simplicity, we show the example with polarization. When the two photons are indistinguishable – all of their mode numbers are identical – the edges that connect vertices *a* and *b* cancel. The remaining green edges with two vertices in *a* or two vertices in *b* show that there are two photons in path *a* or *b*. This is a manifestation of the HOM interference. **C**: In this example, the input photons have orthogonal polarization, and no interference can be observed, thus four possible outputs remain ($H_a V_a$, $H_a V_b$, $V_a H_b$ and $H_b V_b$).

incoming path is replaced by the vertex of the transmitted path. We call this manipulation *BS operation*.

Equipped with complex weights of the graph's edges, we can now naturally investigate interference effects in the graph. As a very prominent example, we analyze how the Hong-Ou-Mandel (HOM) interference [25] manifests itself in the graph (in Fig.2A). For simplicity, phases are represented by colors, e.g. red is 0 and green is $\frac{\pi}{2}$. Each vertex carries a mode label (for example, H/V stands for horizontal/vertical polarization). All the mode numbers of one photon in one path are depicted with a large gray disk. We call such a collection *vertex set*.
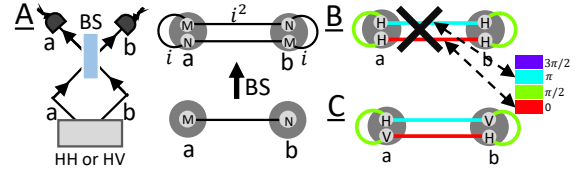
HOM interference can be observed if two indistin-

guishable photons propagate to different input paths of a BS. In Fig.2B, the mode numbers of the two photons are the same and the phases difference is $\pi$, thus the edges cancel each other. In Fig.2C, the two photons have orthogonal mode numbers such as H and V. Therefore the edges do not cancel and no interference is observed.

The action of all other linear optical devices can also be represented in the graph: For example, a phase shifter simply acts as a multiplication of an edge's weight by a complex number and mode shifters change the labels of the vertex. Thus, it is clear that arbitrary experimental setups with non-linear crystals and linear-optical elements – most state-of-the-art photonic experiments – can be described with graphs.

*Computation Complexity and Graphs* — Now we can study prominent linear-optical experiments using graphs. We start with experiments dealing with the boson sampling problem [11–15]. Computing the boson output distribution of a linear network requires the calculation of permanents, which is remarkably difficult, and lies in the complexity class *#P-complete* [27].

In more detail, each boson sampling setup can be described by a unitary matrix $U$, which represents a bipartite graph $G$ (Fig.3A-B). The distribution of outgoing photons can then be calculated by com-
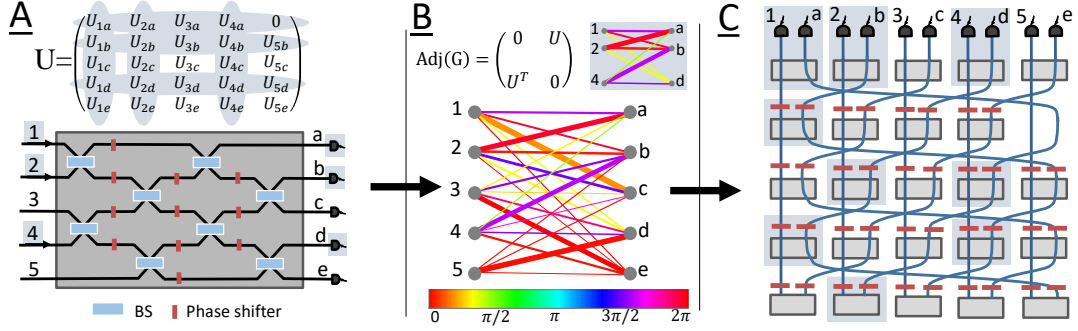
Figure 3. Computation complexity and Graphs. Here we show one graph and two corresponding experimental realizations. **A**: The experimental optical network for Boson sampling described in *Experimental boson sampling* [14]. The linear network is described by a unitary matrix $U$. Each column represents the transition amplitudes from one input to all outputs and each row stands for the transition amplitudes from all inputs to one output. **B**: The unitary matrix can be described as a bipartite graph $G$. The color and width of the edges stand for phases and transition amplitudes, respectively. For example, calculating the perfect matchings of the subgraph highlighted in blue leads to a three-photon coincidence probability in outputs $a$, $b$ and $d$ for inputs 1, 2 and 4. Details are described in supplementary [26]. We can re-interpret this graph as discussed before, where each vertex corresponds to a photon path and each edge represents a crystal. In **C**, the crystal configuration for the bipartite graph $G$ is shown. The subgraph is realized with 9 crystals highlighted with blue background. While in A multi-photonic HOM interference happens, here one observes frustrated multi-pair creation. The matrix $U$ has a zero in $U_{5a}$, because the input in path 5 cannot reach the output $a$, therefore in C the corresponding crystal is missing.

puting perfect matchings of the graph [2]. For a bipartite graph, this corresponds to the calculation of the permanent of the graph's biadjacency matrix (see Fig.3B).

The graph $G$ can also be interpreted as an experiment consisting only of nonlinear crystals [21], shown in Fig.3C. The complex weights stand for the relative complex amplitudes between the generated photon pairs. Calculating the perfect matchings (which is classically difficult) corresponds to measuring n-fold coincidence counts in the output of the crystal network.

Crystal networks can not only represent bipartite graphs but also general undirected graphs. There, enumerating the perfect matchings correspond to calculating the *Hafnian* (which is a generalisation of the Permanent, introduced in [28]). It is unknown how to efficiently approximate the Hafnian [29, 30]. Thus, with experimental setups similar to that in Fig.3C, we can experimentally obtain the result of Hafnians of matrices. The matrix elements can be adjusted by changing the phase shifters and the power of the pump laser. We analyzed the undesired counts from the higher-order emission with the help of [31, 32], and by adapting the laser power the influence on the results remains small [33] (see Supplementary [26]).

In Boson-Sampling setups, multi-photonic HOM interference occurs. In contrast to that, setups of the

form Fig.3C use a new type of interference stemming from a multi-photonic generalization of frustrated down conversion [24] that has never been experimentally observed.

*Restrictions for creating quantum states* — In [21], we have shown a restriction on the generation of high-dimensional GHZ states. The limitation stems from the fact that certain graphs with special properties (concerning their perfect matchings) cannot exist. Since we have extended the use of graphs to linear optics, this restriction applies more generally. In particular, one cannot create a 3- or higher-dimensional GHZ state with more than 4 photons involved. We show this by investigating a particular linear optical experiment.

To understand this example, let's first analyze the 2-dimensional case. For creating 3-particle GHZ state, we can connect two crystals with a PBS. If the two crystals both create an Bell state, a 3-photonic GHZ state with a trigger in $a$ results conditioned on fourfold coincidence counts (shown in Fig.4A) [34]. Extending this to a 4-particle GHZ state, we add another crystal that is connected via a PBS as depicted in Fig.4B).[3]

Now we are trying exactly the same in a 3-dimensional system. To create a 3-dimensional GHZ state, we can use two crystals (where each crystal

---

[2] For technical reasons, generally in BosonSampling experiments ignore cases with more than one photon in a path. In circuits with a sufficiently large number of paths, the cases where each path has at most one photon dominates.

[3] A 4-particle polarization GHZ state can also be created in a simpler way by connecting two crystals via a PBS and not using a trigger. However, we have adapted the example to make the analogy to the 3-dimensional case as accurate as possible.
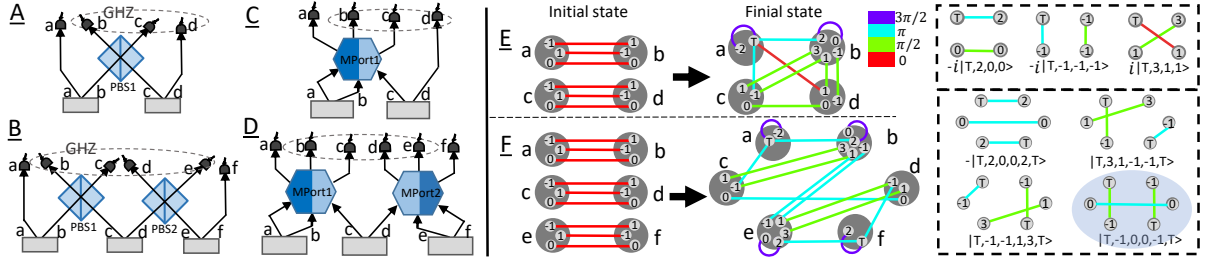
Figure 4. Generating high-dimensional multi-photonic states with linear optical setups. **A**: An optical setup for creating a 2-dimensional 3-photon GHZ-state. In this example, each crystal produces an entangled state $|\psi^+\rangle = 1/\sqrt{2}(|H,H\rangle + |V,V\rangle)$. The photons propagate to a polarizing beam splitter (PBS), and 4-fold coincidence counts lead to a 2-dimensional 3-photon GHZ-state (where the photon in path $a$ acts as a trigger). **B**: For generating high photon number GHZ states, one can add more crystals and connect them via PBSs. **C**: In an analogous way, a 3-dimensional 3-photon GHZ-state has been created recently, by connecting two crystals (each producing a 3-dimensionally entangled photon pair) with a 3-dimensional multi-port (MPort) [10]. **D**: In analogy to B, we now want to extend the setup to create a 3-dimensional GHZ state with 4 particles. However, since this setup uses 6 photons, we expect (due to the result in [21]) to get an additional term in the resulting quantum state. **E**: The graph describing the setup in C, where the *vertex set* (large gray disks) shows the mode numbers of the photons. The initial state shows three connections for each vertex set, which stands for the initial 3-dimensional entanglement (details in the Supplementary [26]). The quantum state conditioned on four-fold coincidences is obtained by calculating the perfect matchings of the graph (described in the dotted box), which lead to a 3-dimensional GHZ-state after triggering the photon in path $a$ on $|T\rangle = 1/\sqrt{2}(|0\rangle + |-1\rangle)$. **F**: The graph which describes the experimental setup in D. As expected, the graph has four perfect matchings, three corresponding to GHZ state while the fourth one (highlighted in blue) is the so-called *Maverick term*.

generates a 3-dimensionally entangled photon pair) and connect them with a 3-dimensional multiport [10], as shown in Fig.4C. In exact analogy to the 2-dimensional case, we add another crystal to the setup, and connect it with another multiport (Fig.4D). As in the 2-dimensional case, we would naturally expect to create a 4-particle GHZ state with this setup, this time however in 3 dimensions.

In this setup, 6 photons are used (two trigger photons and 4 photons for the GHZ state), therefore the corresponding graph has 6 vertices. From [21] we know that such graphs cannot generate high-dimensional GHZ states because additional terms (so-called *Maverick terms*) occur in the final state.[4] And indeed, when we compute the final quantum state, we see that there is an additional perfect matching that leads to the *Maverick term* (Fig.4F). For higher dimensions, even more additional terms will appear – which can be understood by perfect matchings of graphs. If one replaces the probabilistic crystals by deterministic photon-pair sources, then one would get the expected 4-particle GHZ state. The additional term is therefore a genuine manifestation of the graph language in a linear optical quantum experiment.

Finally we show that graph can also help for interpreting quantum protocols. In Fig.5, we show the idea
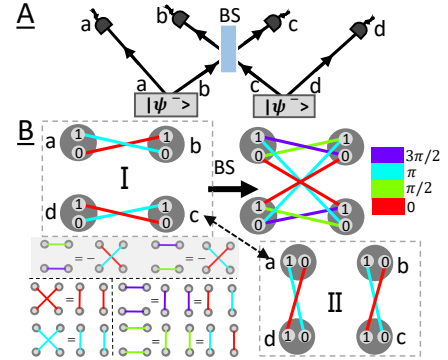


Figure 5. Entanglement swapping and Graphs. **A**: Experimental diagram for entanglement swapping. Each crystal generates an entangled state $|\Psi^-\rangle = \frac{1}{\sqrt{2}}(|0,1\rangle - |1,0\rangle)$. When the photons after the beam splitter emerge in path $b$ and $c$, the two-photon state in $a$ and $d$ is projected into a $|\Psi^-\rangle$. **B**: Here we show the experiment using graphs. The initial $|\Psi^-\rangle$ states (depicted in dotted box I) both have a relative phase of $\pi$, which is represented by edges with different colors (red and blue). Using the *BS operation*, we get the final graph shown on the right side. There are eight perfect matchings, four of them cancel (highlighted in gray). Due to the symmetry in the quantum state (for example, $|0,0,1,1\rangle_{abcd}=|0,1,0,1\rangle_{acbd}$), we rearrange the edges between different vertices after identifying perfect matchings. With $e^{\frac{i3\pi}{2}}e^{\frac{i3\pi}{2}} = e^{i\pi}e^{i2\pi} = e^{i\pi}e^0$, perfect matching of two purple edges can be redescribed as one edge in red and another in blue. The perfect matching for green edges is depicted in the similar way. Finally, we obtain the final graph shown in dotted box II. From the two dotted boxes, we can clearly see the swapping of quantum entanglement.

---

[4] If the quantum state is independent of the trigger photons, then it consists of only four vertices, and these can be in a 3-dimensional GHZ state. Independent means that edges between the trigger vertices and the state vertices do not appear in any perfect matching.

of entanglement swapping [1, 35], which offers an intuitive way to understand this experimental quantum application.

*Conclusion* — We have presented a connection between linear optical quantum experiments with probabilistic sources and graph theory. It shows how to obtain the result of classical difficult mathematic matrix function (Permanent and Hafnian) with quantum experiments. It has only recently been discovered that the conceptually different method called *Gaussian boson sampling* [36] also allows for the investigation of Hafnians [37, 38] – thus understanding the connection between these complementary approaches would be interesting. The underlying effect is *multiphotonic frustrated photon generation*, which would be exciting to see implemented in the laboratories – potentially in integrated platforms which allow for *on-chip* photon pair generation [39–44].

With this connection, we uncovered novel restrictions on classes of quantum states that can be created using state-of-the-art photonic experiments, in particular, GHZ states. The graph-theory-link might as well be used for investigating restrictions of other, much large types of quantum states [45, 46], or could help understanding the (non-) constructability of certain two-dimensional states. Restrictions for the generation of quantum states have been found before, for instance using properties of Fock modes [47], and it would be interesting whether those two independent techniques could be merged. Also severe restrictions on high-dimensional Bell-state measurements are known [48], which limits the application of protocols such as high-dimensional teleportation. The application of the graph-theory-link to such types of quantum measurements would be worthwhile.

We have shown that entanglement swapping can easily be understood with graphs, using the actual experimental implementation. A much more high-level description of such quantum processes has been developed in [49, 50]. A combination of these pictorial approaches could hopefully improve the abstraction and intuitive understanding of these processes.

Graphs have been investigated in other contexts in the realm of quantum physics before, such as in graph states [51, 52] (which can be used for universal quantum computation) or quantum networks [53, 54]. Reinterpretation of these graphs in our language might lead to new concepts for photonic quantum computation.

In [21], we have shown that every experiment (based on crystal configurations as shown in Fig. 1A) corresponds to an undirected graph and vice versa. Here we show that every linear optics setup with non-linear crystals corresponds to an undirected graph with complex weights. It is still open whether for every undirected weighted graph, one can find an experimental setup. This is an important question for the designs of new experiments.

Our method can conveniently describe experiments with probabilistic photon pair sources. It will be useful to understand how the formalism can be extended to other type of probabilistic sources, such as single-photon sources based on weak lasers [55] or three-photon sources based on cascaded down-conversion [56, 57]. Can it also be applied to other (non-photonic) quantum systems with probabilistic source of quanta?

A final, very important question is how to escape the restrictions imposed by the graph-theory link. Deterministic quantum sources [58–60] would need a severe adaption of the description, and active feedforward [61–63] is not known how to be described yet – can they be described with graphs? What are techniques that cannot be described in the way presented here?

[1] Jian-Wei Pan, Zeng-Bing Chen, Chao-Yang Lu, Harald Weinfurter, Anton Zeilinger, and Marek Żukowski. Multiphoton entanglement and interferometry. *Reviews of Modern Physics*, 84(2):777, 2012.
[2] Dik Bouwmeester, Jian-Wei Pan, Matthew Daniell, Harald Weinfurter, and Anton Zeilinger. Observation of three-photon greenberger-horne-zeilinger entanglement. *Physical Review Letters*, 82(7):1345, 1999.
[3] Xing-Can Yao, Tian-Xiong Wang, Ping Xu, He Lu, Ge-Sheng Pan, Xiao-Hui Bao, Cheng-Zhi Peng, Chao-Yang Lu, Yu-Ao Chen, and Jian-Wei Pan. Observation of eight-photon entanglement. *Nature Photonics*, 6(4):225, 2012.
[4] Xi-Lin Wang, Luo-Kan Chen, Wei Li, H-L Huang, Chang Liu, Chao Chen, Y-H Luo, Z-E Su, Dian Wu, Z-D Li, H. Lu, Y. Hu, X. Jiang, C.-Z. Peng, L. Li, N.-L. Liu, Yu-Ao Chen, Chao-Yang Lu, and Jian-Wei Pan. Experimental ten-photon entanglement. *Physical Review Letters*, 117(21):210502, 2016.
[5] Xi-Lin Wang, Yi-Han Luo, He-Liang Huang, Ming-Cheng Chen, Zu-En Su, Chang Liu, Chao Chen, Wei Li, Yu-Qiang Fang, Xiao Jiang, Jun Zhang, Li Li, Nai-

Le Liu, Chao-Yang Lu, and Jian-Wei Pan. 18-qubit entanglement with photon's three degrees of freedom. *arXiv:1801.04043*, 2018.

[6] Manfred Eibl, Nikolai Kiesel, Mohamed Bourennane, Christian Kurtsiefer, and Harald Weinfurter. Experimental realization of a three-qubit entangled w state. *Physical Review Letters*, 92(7):077901, 2004.

[7] Witlef Wieczorek, Roland Krischek, Nikolai Kiesel, Patrick Michelberger, Géza Tóth, and Harald Weinfurter. Experimental entanglement of a six-photon symmetric dicke state. *Physical Review Letters*, 103(2):020504, 2009.

[8] BC Hiesmayr, MJA De Dood, and W Löffler. Observation of four-photon orbital angular momentum entanglement. *Physical Review Letters*, 116(7):073601, 2016.

[9] Mehul Malik, Manuel Erhard, Marcus Huber, Mario Krenn, Robert Fickler, and Anton Zeilinger. Multiphoton entanglement in high dimensions. *Nature Photonics*, 10(4):248, 2016.

[10] Manuel Erhard, Mehul Malik, Mario Krenn, and Anton Zeilinger. Experimental ghz entanglement beyond qubits. *arXiv:1708.03881*, 2017.

[11] Scott Aaronson and Alex Arkhipov. The computational complexity of linear optics. *Proceedings of the forty-third annual ACM symposium on Theory of computing*, page 333, 2011.

[12] Justin B Spring, Benjamin J Metcalf, Peter C Humphreys, W Steven Kolthammer, Xian-Min Jin, Marco Barbieri, Animesh Datta, Nicholas Thomas-Peter, Nathan K Langford, Dmytro Kundys, James C. Gates, Brian J. Smith, Peter G.R. Smith, and Ian A. Walmsley. Boson sampling on a photonic chip. *Science*, 339:798, 2013.

[13] Matthew A Broome, Alessandro Fedrizzi, Saleh Rahimi-Keshari, Justin Dove, Scott Aaronson, Timothy C Ralph, and Andrew G White. Photonic boson sampling in a tunable circuit. *Science*, 339:794, 2013.

[14] Max Tillmann, Borivoje Dakić, René Heilmann, Stefan Nolte, Alexander Szameit, and Philip Walther. Experimental boson sampling. *Nature Photonics*, 7(7):540, 2013.

[15] Andrea Crespi, Roberto Osellame, Roberta Ramponi, Daniel J Brod, Ernesto F Galvao, Nicolo Spagnolo, Chiara Vitelli, Enrico Maiorino, Paolo Mataloni, and Fabio Sciarrino. Integrated multimode interferometers with arbitrary designs for photonic boson sampling. *Nature Photonics*, 7(7):545, 2013.

[16] Jacques Carolan, Christopher Harrold, Chris Sparrow, Enrique Martín-López, Nicholas J Russell, Joshua W Silverstone, Peter J Shadbolt, Nobuyuki Matsuda, Manabu Oguma, Mikitaka Itoh, Graham D. Marshall, Mark G. Thompson, Jonathan C. F. Matthews, Toshikazu Hashimoto, Jeremy L. O'Brien, and Anthony Laing. Universal linear optics. *Science*, 349(6249):711, 2015.

[17] Dik Bouwmeester, Jian-Wei Pan, Klaus Mattle, Manfred Eibl, Harald Weinfurter, and Anton Zeilinger. Experimental quantum teleportation. *Nature*, 390(6660):575, 1997.

[18] Xi-Lin Wang, Xin-Dong Cai, Zu-En Su, Ming-Cheng Chen, Dian Wu, Li Li, Nai-Le Liu, Chao-Yang Lu, and Jian-Wei Pan. Quantum teleportation of multiple degrees of freedom of a single photon. *Nature*, 518(7540):516, 2015.

[19] Jian-Wei Pan, Dik Bouwmeester, Harald Weinfurter, and Anton Zeilinger. Experimental entanglement swapping: entangling photons that never interacted. *Physical Review Letters*, 80(18):3891, 1998.

[20] Yingwen Zhang, Megan Agnew, Thomas Roger, Filippus S Roux, Thomas Konrad, Daniele Faccio, Jonathan Leach, and Andrew Forbes. Simultaneous entanglement swapping of multiple orbital angular momentum states of light. *Nature Communications*, 8(1):632, 2017.

[21] Mario Krenn, Xuemei Gu, and Anton Zeilinger. Quantum experiments and graphs: Multiparty states as coherent superpositions of perfect matchings. *Physical Review Letters*, 119(24):240403, 2017.

[22] Mario Krenn, Mehul Malik, Robert Fickler, Radek Lapkiewicz, and Anton Zeilinger. Automated search for new quantum experiments. *Physical Review Letters*, 116(9):090405, 2016.

[23] Mario Krenn, Armin Hochrainer, Mayukh Lahiri, and Anton Zeilinger. Entanglement by path identity. *Physical Review Letters*, 118(8):080401, 2017.

[24] TJ Herzog, JG Rarity, H Weinfurter, and A Zeilinger. Frustrated two-photon creation via interference. *Physical Review Letters*, 72(5):629, 1994.

[25] Chong-Ki Hong, Zhe-Yu Ou, and Leonard Mandel. Measurement of subpicosecond time intervals between two photons by interference. *Physical Review Letters*, 59(18):2044, 1987.

[26] Supplementary.

[27] Leslie G Valiant. The complexity of computing the permanent. *Theoretical computer science*, 8(2):189, 1979.

[28] Eduardo R Caianiello. On quantum field theory-i: explicit solution of dyson's equation in electrodynamics without use of feynman graphs. *Il Nuovo Cimento (1943-1954)*, 10(12):1634, 1953.

[29] Andreas Björklund. Counting perfect matchings as fast as ryser. *Proceedings of the twenty-third annual ACM-SIAM symposium on Discrete Algorithms*, page 914, 2012.

[30] Alexander Barvinok. Approximating permanents and hafnians. *Discrete Analysis*, 2, 2017.

[31] LJ Wang, XY Zou, and L Mandel. Induced coherence without induced emission. *Physical Review A*, 44(7):4614, 1991.

[32] Mayukh Lahiri, Radek Lapkiewicz, Gabriela Barreto Lemos, and Anton Zeilinger. Theory of quantum imaging with undetected photons. *Physical Review A*, 92(1):013832, 2015.

[33] HM Wiseman and Klaus Mølmer. Induced coherence with and without induced emission. *Physics Letters A*, 270(5):245, 2000.

[34] Jian-Wei Pan, Matthew Daniell, Sara Gasparoni, Gregor Weihs, and Anton Zeilinger. Experimental demonstration of four-photon entanglement and high-fidelity teleportation. *Physical Review Letters*, 86(20):4435, 2001.

[35] Marek Zukowski, Anton Zeilinger, Michael A Horne, and Aarthur K Ekert. "event-ready-detectors" bell experiment via entanglement swapping. *Physical Review Letters*, 71:4287, 1993.

[36] AP Lund, A Laing, S Rahimi-Keshari, T Rudolph, Jeremy L O'Brien, and TC Ralph. Boson sam-

pling from a gaussian state. *Physical Review Letters*, 113(10):100502, 2014.

[37] Craig S Hamilton, Regina Kruse, Linda Sansoni, Sonja Barkhofen, Christine Silberhorn, and Igor Jex. Gaussian boson sampling. *Physical Review Letters*, 119(17):170501, 2017.

[38] Kamil Brádler, Pierre-Luc Dallaire-Demers, Patrick Rebentrost, Daiqin Su, and Christian Weedbrook. Gaussian boson sampling for perfect matchings of arbitrary graphs. *arXiv:1712.06729*, 2017.

[39] H Jin, FM Liu, P Xu, JL Xia, ML Zhong, Y Yuan, JW Zhou, YX Gong, W Wang, and SN Zhu. On-chip generation and manipulation of entangled photons based on reconfigurable lithium-niobate waveguide circuits. *Physical Review Letters*, 113(10):103601, 2014.

[40] Joshua W Silverstone, Damien Bonneau, Kazuya Ohira, Nob Suzuki, Haruhiko Yoshida, Norio Iizuka, Mizunori Ezaki, Chandra M Natarajan, Michael G Tanner, Robert H Hadfield, V. Zwiller, G. D. Marshall, J. G. Rarity, J. L. O'Brien, and M. G. Thompson. On-chip quantum interference between silicon photon-pair sources. *Nature Photonics*, 8(2):104, 2014.

[41] Joshua W Silverstone, Raffaele Santagati, Damien Bonneau, Michael J Strain, Marc Sorel, Jeremy L O'Brien, and Mark G Thompson. Qubit entanglement between ring-resonator photon-pair sources on a silicon chip. *Nature Communications*, 6:7948, 2015.

[42] Stephan Krapick, Benjamin Brecht, Harald Herrmann, Viktor Quiring, and Christine Silberhorn. On-chip generation of photon-triplet states. *Optics Express*, 24(3):2836, 2016.

[43] Lan-Tian Feng, Ming Zhang, Yang Chen, Guo-Ping Guo, Guang-Can Guo, Dao-Xin Daiy, and Xi-Feng Ren. On-chip transverse-mode entangled photon source. *arXiv:1802.09847*, 2018.

[44] Jianwei Wang, Stefano Paesani, Yunhong Ding, Raffaele Santagati, Paul Skrzypczyk, Alexia Salavrakos, Jordi Tura, Remigiusz Augusiak, Laura Mančinska, Davide Bacco, Davide Bacco, Damien Bonneau, Joshua W. Silverstone, Qihuang Gong, Antonio Acin, Karsten Rottwitt, Leif K. Oxenlowe, Jeremy L. O'Brien, Anthony Laing, and Mark G. Thompson. Multidimensional quantum entanglement with large-scale integrated optics. *Science*, page eaar7053, 2018.

[45] Marcus Huber and Julio I de Vicente. Structure of multidimensional entanglement in multipartite systems. *Physical Review Letters*, 110(3):030501, 2013.

[46] Dardo Goyeneche, Jakub Bielawski, and Karol Życzkowski. Multipartite entanglement in heterogeneous systems. *Physical Review A*, 94(1):012346, 2016.

[47] Piotr Migdał, Javier Rodríguez-Laguna, Michał Oszmaniec, and Maciej Lewenstein. Multiphoton states related via linear optics. *Physical Review A*, 89(6):062329, 2014.

[48] John Calsamiglia. Generalized measurements by linear elements. *Physical Review A*, 65(3):030301, 2002.

[49] Bob Coecke. Kindergarten quantum mechanics: Lecture notes. *AIP Conference Proceedings*, 810(1):81, 2006.

[50] Samson Abramsky and Bob Coecke. A categorical semantics of quantum protocols. *Logic in computer science, 2004. Proceedings of the 19th Annual IEEE Symposium on*, page 415, 2004.

[51] Robert Raussendorf and Hans J Briegel. A one-way quantum computer. *Physical Review Letters*, 86(22):5188, 2001.

[52] Marc Hein, Wolfgang Dür, Jens Eisert, Robert Raussendorf, M Nest, and H-J Briegel. Entanglement in graph states and its applications. *quant-ph/0602096*, 2006.

[53] Sébastien Perseguers, Maciej Lewenstein, A Acín, and J Ignacio Cirac. Quantum random networks. *Nature Physics*, 6(7):539, 2010.

[54] Martí Cuquet and John Calsamiglia. Entanglement percolation in quantum complex networks. *Physical Review Letters*, 103(24):240503, 2009.

[55] Zhi Zhao, Yu-Ao Chen, An-Ning Zhang, Tao Yang, Hans J Briegel, and Jian-Wei Pan. Experimental demonstration of five-photon entanglement and open-destination teleportation. *Nature*, 430(6995):54, 2004.

[56] Hannes Hübel, Deny R Hamel, Alessandro Fedrizzi, Sven Ramelow, Kevin J Resch, and Thomas Jennewein. Direct generation of photon triplets using cascaded photon-pair sources. *Nature*, 466(7306):601, 2010.

[57] Deny R Hamel, Lynden K Shalm, Hannes Hübel, Aaron J Miller, Francesco Marsili, Varun B Verma, Richard P Mirin, Sae Woo Nam, Kevin J Resch, and Thomas Jennewein. Direct generation of three-photon polarization entanglement. *Nature Photonics*, 8(10):801, 2014.

[58] Charles Santori, David Fattal, Jelena Vučković, Glenn S Solomon, and Yoshihisa Yamamoto. Indistinguishable photons from a single-photon device. *Nature*, 419(6907):594, 2002.

[59] P Michler, A Kiraz, C Becher, WV Schoenfeld, PM Petroff, Lidong Zhang, E Hu, and A Imamoglu. A quantum dot single-photon turnstile device. *Science*, 290(5500):2282, 2000.

[60] Pascale Senellart, Glenn Solomon, and Andrew White. High-performance semiconductor quantum-dot single-photon sources. *Nature Nanotechnology*, 12(11):1026, 2017.

[61] S Giacomini, F Sciarrino, E Lombardi, and F De Martini. Active teleportation of a quantum bit. *Physical Review A*, 66(3):030302, 2002.

[62] TB Pittman, BC Jacobs, and JD Franson. Demonstration of feed-forward control for linear optics quantum computation. *Physical Review A*, 66(5):052305, 2002.

[63] Xiao-Song Ma, Thomas Herbst, Thomas Scheidl, Daqing Wang, Sebastian Kropatschek, William Naylor, Bernhard Wittmann, Alexandra Mech, Johannes Kofler, Elena Anisimova, Vadim Makarov, Thomas Jennewein, Rupert Ursin, and Anton Zeilinger. Quantum teleportation over 143 kilometres using active feed-forward. *Nature*, 489(7415):269, 2012.

[64] Jonathan Leach, Miles J Padgett, Stephen M Barnett, Sonja Franke-Arnold, and Johannes Courtial. Measuring the orbital angular momentum of a single photon. *Physical Review Letters*, 88(25):257901, 2002.

# Supplemental Materials

## I.  APPENDIX I. COMPUTATION COMPLEXITY AND PERFECT MATCHINGS
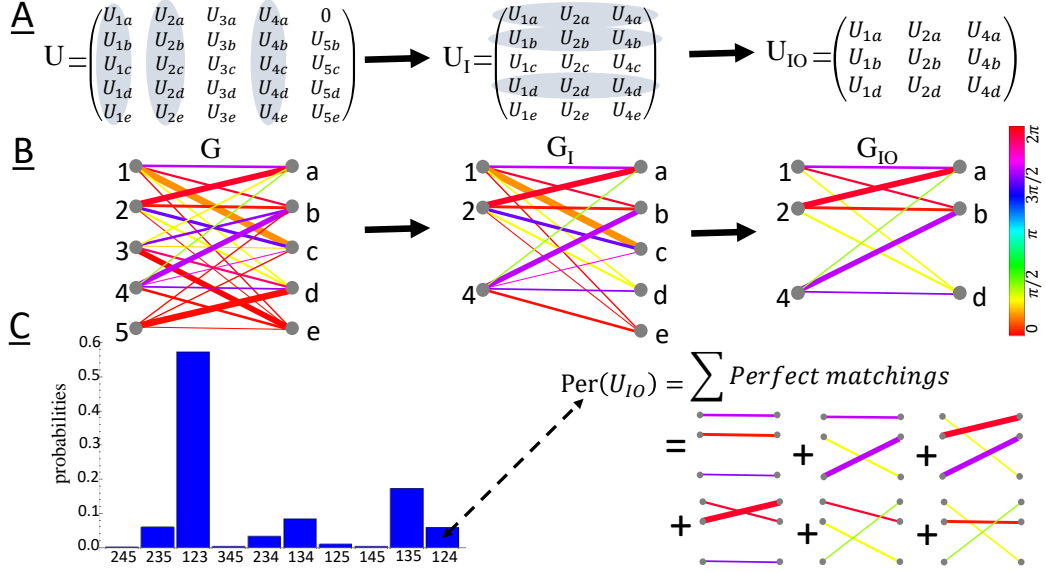
### A.   Permanent of Submatrix



Figure 6. Boson Sampling and Perfect Matchings. **A**: The unitary matrix $U$ for the linear network shown in *Experimental boson sampling* [14]. Each column represents an input and each row stands for one output. As an example, we choose three inputs (1, 2, 4) and then measure three outputs ($a$, $b$, $d$). Computing the probability of the output distribution requires calculating the permanent of the sub-matrix $U_{IO}$, which cannot be done efficiently. **B**: The matrix $U$ represents a bipartite graph $G$. The color and width of the edges stand for phases and probability amplitudes, respectively. Enumerating the perfect matchings of the subgraph $G_{IO}$ gives the output probability amplitude. **C**: Experimental result for the boson sampling. In our specific example (inputs: 1, 2, 4; outputs: $a$, $b$, $d$), we obtain six perfect matchings in the sub-graph $G_{IO}$. The sum of these perfect matchings leads to the output probability amplitude.

The unitary matrix $U$ (in Fig.6A) for the linear optical network is presented in main text (which has been used in the experiment [14]):

$$U = \begin{pmatrix} 0.0776 - 0.2522i & -0.8878 + 0.1067i & 0.0843 + 0.1724i & -0.0189 - 0.3056i & 0 \\ 0.2214 - 0.0442i & -0.2936 - 0.0593i & 0.0503 - 0.3352i & -0.2778 + 0.7671i & 0.2802 \\ -0.6981 - 0.5741i & 0.0653 - 0.2926i & 0.0892 + 0.091i & -0.0748 + 0.0852i & 0.2527 \\ 0.0913 + 0.1746i & 0.0525 + 0.1004i & -0.2432 + 0.0786i & 0.0151 - 0.2622i & 0.9021 \\ 0.1531 & 0.088 & 0.8755 & 0.3982 & 0.2087 \end{pmatrix} \quad (1)$$

Each column stands for one input and each row represents one output. In our example, photons enter into the inputs (1, 2, 4). Therefore, we can extract the sub-matrix $U_I$ from matrix $U$

$$U_I = \begin{pmatrix} 0.0776 - 0.2522i & -0.8878 + 0.1067i & -0.0189 - 0.3056i \\ 0.2214 - 0.0442i & -0.2936 - 0.0593i & -0.2778 + 0.7671i \\ -0.6981 - 0.5741i & 0.0653 - 0.2926i & -0.0748 + 0.0852i \\ 0.0913 + 0.1746i & 0.0525 + 0.1004i & 0.0151 - 0.2622i \\ 0.1531 & 0.088 & 0.3982 \end{pmatrix} \quad (2)$$

When we measure three outputs $(a, b, d)$, we obtained the finial $3{\times}3$ sub-matrix $U_{IO}$ which is

$$U_{IO} = \begin{pmatrix} 0.0776 - 0.2522i & -0.8878 + 0.1067i & -0.0189 - 0.3056i \\ 0.2214 - 0.0442i & -0.2936 - 0.0593i & -0.2778 + 0.7671i \\ 0.0913 + 0.1746i & 0.0525 + 0.1004i & 0.0151 - 0.2622i \end{pmatrix} \tag{3}$$

The output probability amplitude can be obtained by computing the permanent of matrix $U_{IO}$. The unitary matrix $U$ corresponds to a bipartite graph $G$ which is described in Fig.6B. Enumerating the perfect matchings of subgraph $G_{IO}$ is the same to computing the permanent of matrix $U_{IO}$.

## B.  Down-conversion crystal network

The graph can be interpreted as a crystal network [21]. In boson sampling setups, the interference comes from multi-photon HOM effect, while in the crystal networks the interference stems from multi-photon frustrated photon creation. The down-conversion process can be described as an operation [31, 32] in the form of

$$\hat{U}_{a,b} = \sum_{n=0}^{\infty} \frac{g^n}{n!} (\hat{a}_a^\dagger \hat{a}_b^\dagger - \hat{a}_a \hat{a}_b)^n \tag{4}$$

where $\hat{a}_a^\dagger$ and $\hat{a}_a$ are creation and annihilation operators for a photon in path $a$, and $g$ is proportional to the down-conversion rate and pump power. Therefore, the quantum state can be expressed as $|\psi\rangle = \hat{U}_{a,b}|vac\rangle$, where $|vac\rangle$ is the vacuum state.

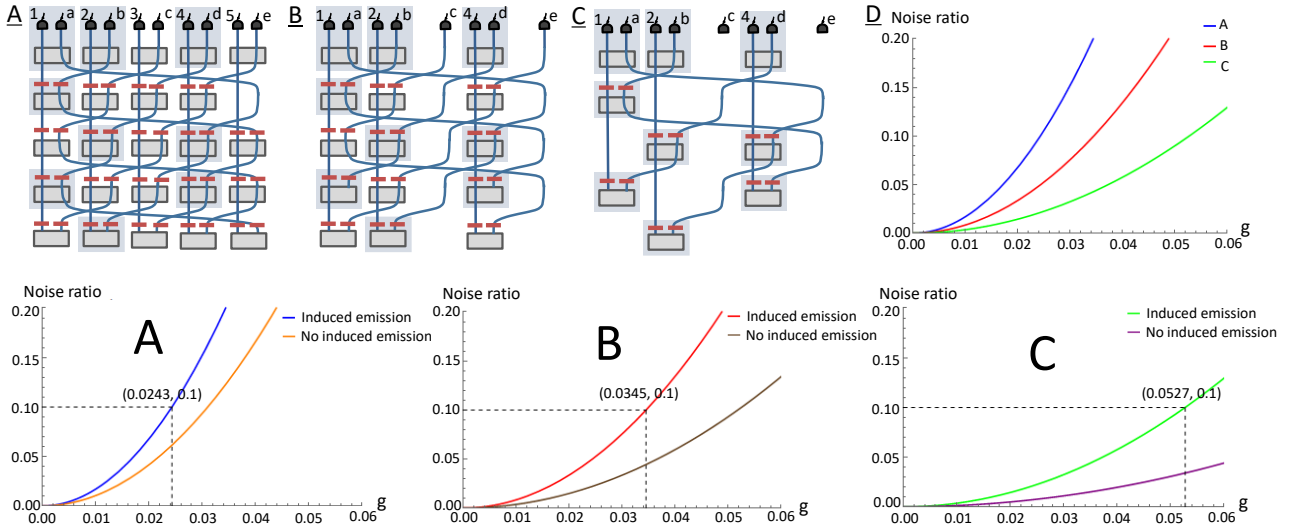To analyze the noise, we theoretically calculate the setups (Fig.7A, B and C) with the help of [31].



Figure 7. The influence of induced emission. **A**, **B**, **C**: Crystal setups represented by the bipartite graphs $G$, $G_I$, $G_{IO}$ in Fig.6B. Below we show the noise (i.e. additional undesired noise), and the proportion which arises due to induced emission. **D**: Noise ratio of the three setups.

## II. APPENDIX II. DETAILS OF THE MULTIPORT EXPERIMENT AND GRAPH

Here we describe the experiment for creating 3-dimensional GHZ-state in detail and give a explicit description step by step with the graph in Fig.8.
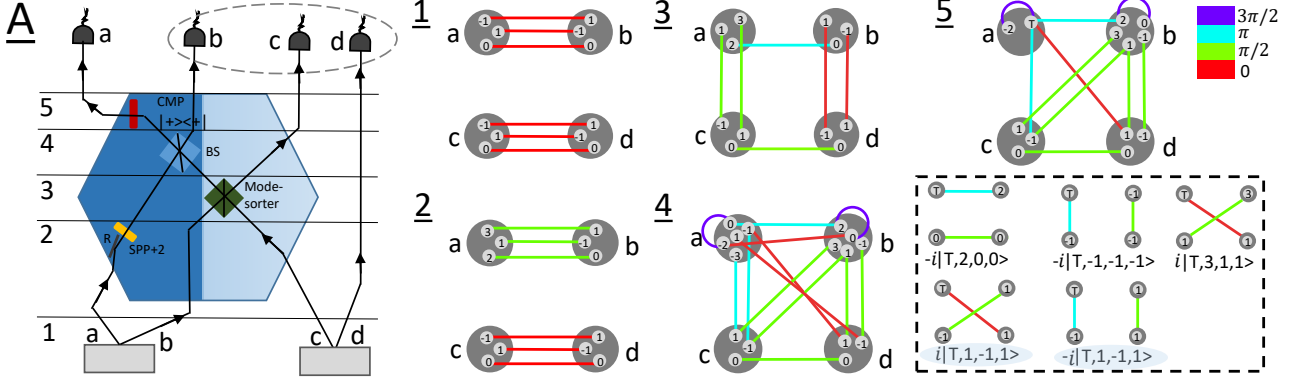


Figure 8. Multiport experiment and Graph. **A**: An experimental setup for producing a 3-dimensional GHZ-state presented in *Experimental GHZ Entanglement beyond Qubits* [10]. Each crystal produces a maximally 3-dimensional entangled state $1/\sqrt{3}(|0,0\rangle + |-1,1\rangle + |1,-1\rangle)$. The multiport (originate from [10]) consists of a reflection (R), a spiral-phase-plate (SPP), a beam splitter, an orbital angular momentum (OAM) mode sorter [64] and a coherent mode-projection (CMP). In the graph, each vertex carries a label which stands for the mode number (such as 0, 1, −1). The *vertex set* (described with a large gray disk) represents one photon path. Each edge shows a photon pair correlation. The color and width of the edge stands for the phase and probability amplitude. The experiment can be described in the following five steps. **Step 1**: two crystals produce 3-dimensional 2-photon state between path $a$ and $b$ and path $c$ and $d$ respectively. Therefore the initial state is described by three edges connected with *vertex set* $a$ and $b$ and *vertex set* $c$ and $d$. **Step 2**: When the photon propagates through $R$ and $SPP$, the mode numbers will change as $|\ell\rangle \to |-\ell+2\rangle$ with an additional phase $\pi/2$. This process can be described by altering the label of vertices in the *vertex set* and the color of related edges. **Step 3**: The action of OAM sorter in graph. The mode sorter separates incoming photons according to theirs OAM value. Even modes will reflect with a phase $\pi/2$ and odd modes will transmit (for example, the mode of a photon in path $c$ propagating to the sorter will change as follows: even mode: $|\ell\rangle_c \to |-\ell\rangle_c$; odd mode: $|\ell\rangle_c \to |\ell\rangle_b$.). Therefore in the graph, vertices carrying even labels in *vertex set* $c$ will change the sign of the label and the connected edges get an additional complex weight $i$. Vertices carrying the odd labels in *vertex set* $c$ will go to path $b$, therefore their edges $E_{cd}$ are transferred to $E_{bd}$. The photon in path $b$ propagates to OAM sorter in an analogous way. **Step 4**: When a photon in path $a$ enters the beam splitter, it either reflects to path $a$ with a phase $\pi/2$ or transmits to path $b$. With this *BS operation*, the vertices in $a$ and $b$ will change labels and the original edges would get an additional complex weight $i$. **Step 5**: The photon in path $a$ will pass through a coherent mode-projection (CMP), which project the state $|0\rangle + |-1\rangle$ into state $|T\rangle$. This is described by changing the labels 0 or −1 of vertex in path $a$ to $T$. Finally, four-fold coincidence counts requires enumerating perfect matchings of the graph (depicted in dotted box). The quantum state for the experiment is $(-|2,0,0\rangle - |-1,-1,-1\rangle + |3,1,1\rangle)_{bcd}$, which can be rewritten in $(-|0,0,0\rangle - |1,1,1\rangle + |2,2,2\rangle)_{bcd}$ with some local operation.

## A. Details of the six-photon quantum experiment

Here we show details for the experiment (see Fig4.D in the main text), which is expected to create an 3-dimensional GHZ-state at first sight. However, as known from [21], the graph has four perfect matchings, three corresponding to GHZ state while the fourth one (highlighted in blue) is the so-called *Maverick term*.
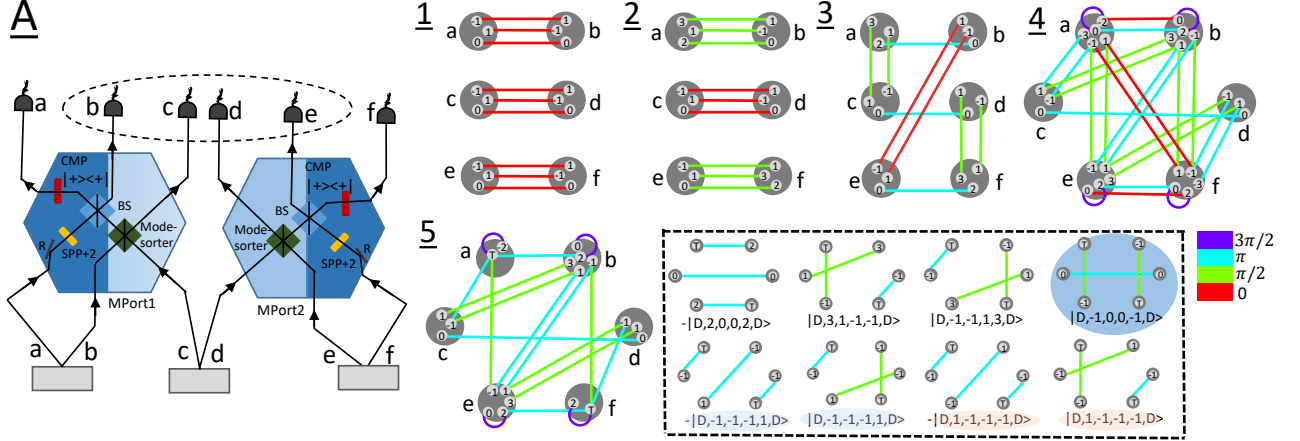


Figure 9. Restrictions on creation of quantum states. **A**: A setup to apparently create a 3-dimensional GHZ-state with 6 particles. Photons in paths $a$, $b$ and $c$ go to MPort1 and others in paths $d$, $e$ and $f$ go to MPort2. This experimental arrangement is analogous to Fig.4B in main text. **Step 1**: Three crystals produce the 3-dimensional 2-photon pairs in paths $a$, $b$, $c$, $d$, $e$ and $f$. Therefore the initial state is described by six edges connected with the corresponding *vertex sets*. **Step 2**: The photons in path $a$ and $f$ go through a $R$ and $SPP$. In the graph language, this operation will change labels of vertices and colors of edges of the graph, respectively. **Step 3**: Photons in path $b$ and path $c$ propagate to a OAM mode sorter, the same as photons in the path $d$ and $e$. Similar to Step 3 in Fig.8. **Step 4**: The photon in path $a$ will reflect to path $a$ with a phase $\pi/2$ or transmit to path $b$, which is similar to photon in path $b$, $e$ and $f$. With this *BS operation*, the labels of the relevant vertices will change and the original edges get an additional complex weight $i$. **Step 5**: With the projection, we remove all vertices which do not carry the labels (0 and $-1$). The triggered vertices are renamed to label $T$. With that, we obtain the final graph of the setup. With six-fold coincidence counts, we calculate the perfect matching of the graph. There are eight perfect matchings (depicted in dotted box) where four of them cancel. After triggering photons in path $a$ and $f$, the result state is $(-|2,0,0,2\rangle + |3,1,-1,-1\rangle + |-1,-1,1,3\rangle + |-1,0,0,-1\rangle)_{bcde}$, which is a 3-dimensional four-photon GHZ-state with the *Maverick term* $|-1,0,0,-1\rangle_{bcde}$.